International Journal of Sustainable Development and Planning
Vol. 20, No. 11, November, 2025, pp. 4679-4690
Journal homepage: http://iieta.org/journals/ijsdp

Predicting Urban Growth in Disaster-Prone Areas with CA-Markov Modelling on Batu City, East Java

Mohammad Reza[1*], Batara Surya[2], Arifuddin Akil[3], Muhamad Arif Nasution[4], Murshal Manaf[2]

[1] Department of Urban and Regional Planning, Faculty of Civil and Planning, National Institute of Technology, Malang City 65145, Indonesia
[2] Department of Urban and Regional Planning, Faculty of Engineering, Bosowa University, Makassar City 90231, Indonesia
[3] Department of Urban and Regional Planning, Faculty of Engineering, Hasanuddin University, Makassar City 90245, Indonesia
[4] Agrotechnology Study Program, Faculty of Agriculture, Bosowa University, Makassar City 90231, Indonesia

Corresponding Author Email: mohammad_reza@lecturer.itn.ac.id

https://doi.org/10.18280/ijsdp.201112

Received: 21 August 2025
Revised: 1 October 2025
Accepted: 6 November 2025
Available online: 30 November 2025

Keywords:
cellular automata, disaster prone areas, land commodification

ABSTRACT

Rapid urban expansion in Batu City has triggered extensive land conversion, primarily from agricultural to residential uses, driven by population growth and land commodification. This study aims to analyze and predict land cover dynamics from 2013 to 2043 using multi-temporal Landsat 8 and Sentinel 2A imagery integrated with the Cellular Automata Markov (CA-Markov) model. The analysis reveals a 35% decline in agricultural areas and an 86% increase in residential areas over the past decade, while forest and shrubland have slightly decreased. These changes illustrate the growing pressure of urban development on productive land resources. Overlaying land cover data with the disaster-prone map indicates that approximately 27% of Batu City's territory lies within hazard-prone areas, dominated by landslide (20%) and volcanic (4%) zones. Around 20% of new residential development is concentrated in medium to high-risk zones, particularly in the eastern and northern regions of Batu and Bumiaji Districts. The CA-Markov projection suggests continued urban expansion toward these vulnerable zones by 2043 if no spatial control policies are implemented. The novelty of this study lies in integrating CA-Markov simulation with quantitative disaster-risk assessment, providing valuable insights for promoting disaster-resilient land-use planning and sustainable urban development in rapidly growing regions.

1. INTRODUCTION

Urbanization has emerged as one of the defining processes of the 21st century, reshaping global landscapes and socio-economic structures. More than half of the world's population now resides in urban areas, and this figure is projected to reach 70% by 2050 [1-3]. This demographic shift has resulted in the massive expansion of built-up areas and the intensification of land competition between agricultural, residential, and industrial uses [4]. Between 1985 and 2015, the world's urban areas nearly tripled, indicating not only population concentration but also the spatial manifestation of economic and political forces that drive cities toward relentless physical growth [5].

However, such expansion is often spatially unbalanced. In many developing regions, particularly Southeast Asia, urban growth occurs without adequate planning or environmental consideration [6]. Land is no longer valued solely for its ecological and productive functions but increasingly as a tradable commodity. The commodification of land and the transformation of land into an economic asset for speculation, tourism, or real estate development has become a central driver of spatial change in many peri-urban and agricultural areas [7-10]. This process redefines land ownership and use, leading to a structural shift from agrarian-based livelihoods toward capital-oriented urban economies.

In Indonesia, this phenomenon is clearly visible in cities undergoing rapid economic transformation. The combination of tourism, investment, and infrastructure development has accelerated the conversion of agricultural land into built-up areas, often beyond the carrying capacity of the local environment [11]. The *post-decentralization* era has further intensified this dynamic, as regional governments seek to attract private investment through land-use flexibility and urban expansion incentives. Consequently, agricultural lands, which traditionally served as a source of local food security and ecological stability, have been converted into residential and commercial zones.

Batu City in East Java is a representative case of this transformation. Historically, Batu City was known as a highland agropolitan area with fertile volcanic soils, supporting vegetable and fruit cultivation as the backbone of its local economy. Yet, since the early 2000s, the city's rapid growth in tourism and real estate has led to significant land

conversion. Tourism-driven urbanization, supported by improved accessibility and the rise of the Malang Metropolitan Area, has increased demand for accommodation, resorts, and secondary housing. As a result, many productive farmlands have been transformed into urban settlements, particularly in Bumiaji, Batu, and Junrejo districts, areas where land values have sharply increased due to market speculation and tourism investment.

This land commodification process is not only altering Batu's spatial structure but also creating environmental and disaster-related risks. The city is situated on complex volcanic and mountainous terrain, influenced by Mount Arjuno and Mount Panderman, which makes it highly susceptible to landslides, floods, and volcanic hazards. Previous spatial analyses have indicated that approximately 27% of Batu's total area falls within moderate to high disaster-prone zones [12]. Ironically, these are also the same areas where land conversion for housing and tourism occurs most intensively. The expansion of impermeable surfaces and deforestation of steep slopes further exacerbate the risk of hydrometeorological disasters.

The overlapping of urban growth and disaster exposure reveals a critical weakness in spatial governance. Existing spatial plans (*RTRW Batu City 2021-2040*) have not fully integrated dynamic land-use modeling or risk-based zoning. Furthermore, urban expansion is often treated as an inevitable sign of progress rather than a process requiring ecological balance and risk consideration. As a result, disaster risk management tends to be reactive rather than preventive, focusing on post-event recovery instead of spatial anticipation.

From an academic perspective, research on Batu City has primarily focused on either (1) land-use change and agricultural decline or (2) disaster-prone area mapping. Few studies have attempted to integrate both dimensions into a single predictive modeling framework that can simulate future urban expansion in relation to disaster risk. This gap limits policymakers' ability to foresee potential conflicts between development and environmental safety.

The CA-Markov (Cellular Automata Markov Chain) model offers a robust methodological solution for this challenge. The Markov Chain component estimates the probability of land transitions based on historical patterns, while the cellular automata component spatially allocates these transitions considering neighborhood effects and spatial constraints. Together, they allow for dynamic simulation of urban growth and scenario-based prediction of land-use changes. When combined with hazard maps, CA-Markov analysis can identify potential future overlaps between built-up expansion and disaster-prone zones, providing a scientific foundation for risk-sensitive urban planning.

Therefore, this study aims to:

- Analyze the spatio-temporal changes in land use and land cover (LULC) in Batu City between 2013 and 2023.
- Predict the spatial distribution of urban expansion up to 2043 using the CA-Markov model.

By addressing these objectives, this research seeks to contribute both theoretically and practically. Theoretically, it advances the understanding of land commodification as a driver of spatial risk accumulation, a concept that connects urban economic dynamics with ecological vulnerability. Practically, it provides policymakers and planners with quantitative evidence to refine spatial plans, enforce zoning control, and strengthen disaster prevention strategies.

Ultimately, the findings of this study are expected to guide the development of resilient and sustainable urban planning in Batu City. Integrating predictive modeling with disaster-risk assessment can support the formulation of adaptive land-use policies, balancing economic growth with environmental safety. Moreover, this approach can be replicated in other mid-sized Indonesian cities that experience similar pressures of tourism-based urbanization and agricultural land conversion.

2. MATERIAL AND METHODS

This study employs a spatial analysis approach supported by remote sensing and geographic information system (GIS) techniques using ArcGIS 10.8 and IDRISI TerrSet software. The overall methodological framework consists of four main stages: data collection, image preprocessing, land use classification and validation, and land use change prediction using the CA-Markov model.

2.1 Study area

Batu City, located in East Java Province, Indonesia, lies between 7°44′55″–7°49′04″ S and 112°30′50″–112°35′50″ E. It covers approximately 199.09 km² and is characterized by steep slopes (15–40%), volcanic soils, and high rainfall. These conditions make the area both agriculturally productive and highly prone to natural hazards such as landslides and floods in Figure 1.

2.2 Data collection

The research utilized a combination of remote sensing and secondary spatial data. Satellite imagery:

- Landsat 8 OLI (acquired in 2013 and 2016) with a spatial resolution of 30m [13].
- Sentinel-2A MSI (acquired in 2017 and 2023) with a spatial resolution of 10m [14].

Supporting spatial data: administrative boundaries, slope, elevation, and disaster-prone areas derived from Bappeda and BPBD Batu City [15]. All data were reprojected into UTM Zone 49S and WGS 84, using ArcGIS 10.8.

2.3 Image preprocessing

To ensure data comparability between different sensors, several preprocessing steps were applied before classification.

- Atmospheric correction
  Atmospheric effects were corrected using the Dark Object Subtraction (DOS) method in *ENVI 5.6*, which adjusts for haze and scattering by normalizing pixel values [16]. This process improves the radiometric consistency between multi-temporal images [16].
- Geometric correction and subsetting
  All imagery was geometrically corrected using ground control points (GCPs) [17] and adjusted to match the administrative boundary of Batu City. Subsetting was performed to crop the study area from each scene [18].
- Cloud masking and thresholds
  Only images with less than 10% cloud cover were selected to minimize noise in classification. The *Quality Assessment (QA)* band in Landsat 8 and the

Scene Classification Layer (SCL) in Sentinel-2A were used to mask cloud and cirrus pixels [19].

- Spatial harmonization (resampling)
  Because Landsat 8 has a 30 m resolution while Sentinel-2A has 10 m, the Sentinel imagery was resampled to 30m using the nearest neighbor interpolation method to maintain spectral fidelity and ensure pixel compatibility for temporal comparison. This harmonization allowed accurate overlay and change detection in ArcGIS and TerrSet [20].
- Band Combination and enhancement
  False-color composites (bands 5-4-3 for Landsat 8 and 8-4-3 for Sentinel-2A) were used to enhance vegetation and built-up area separability [21, 22].

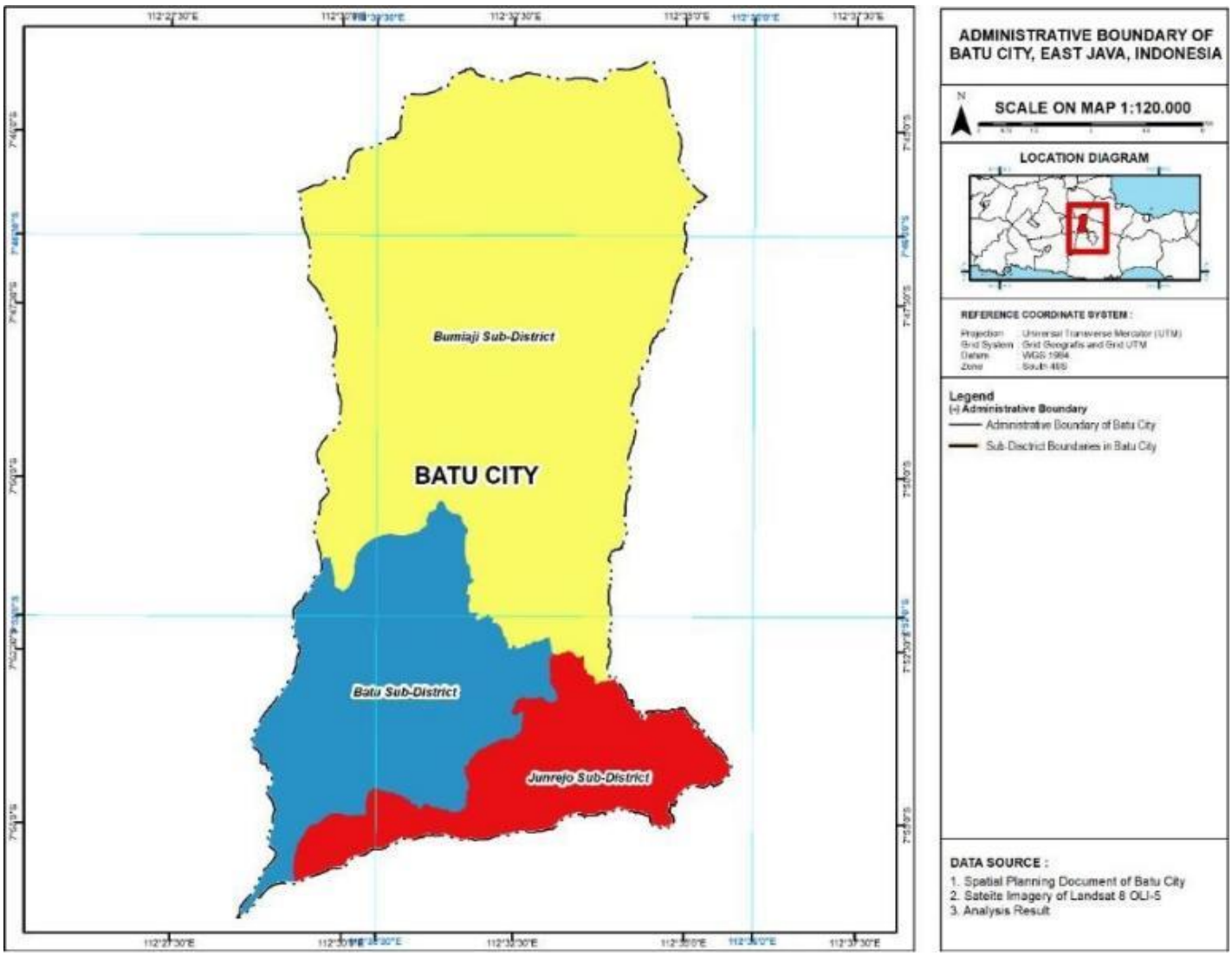

Figure 1. Map of Batu City

2.4 Land use classification and accuracy assessment

Supervised classification using the Maximum Likelihood Classifier (MLC) was applied to categorize land use into 4 major classes [23-25]:

- Agricultural land
- Water Bodies
- Seatlemen Area
- Built-up Areas
- Forest
- Shrubland

Training samples were derived from field validation points and high-resolution imagery. Classification accuracy was evaluated through a confusion matrix and Kappa coefficient, yielding an overall accuracy of 87% for 2013 and 89% for 2023, both exceeding the minimum threshold (≥ 85%) recommended in Figure 2 [26].

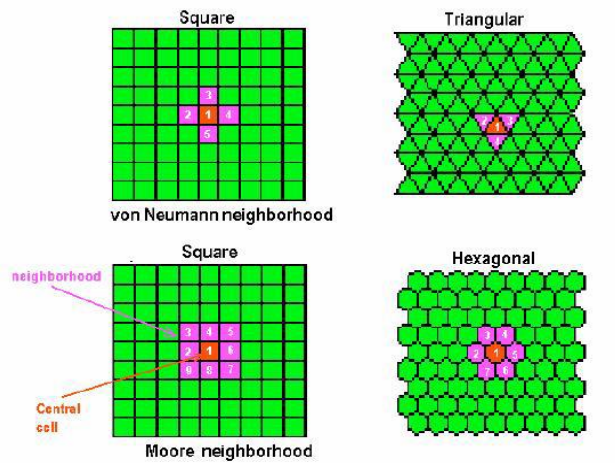

Figure 2. Central cells representing 2D cellular automata [27]

2.5 Land use change detection

Land cover maps for 2013 and 2023 were compared using post-classification comparison in ArcGIS. The CrossTab function calculated the area (in hectares) and percentage change for each land use class. The analysis revealed the spatial distribution and rate of conversion from agricultural to residential use.

2.6 CA-Markov modeling for land cover projection

Future land use for the year 2043 was simulated using the CA-Markov model in TerrSet 2020 (Clark Labs).

- Markov chain analysis estimated transition probabilities from the 2019-2023 period.
- Cellular automata (CA) spatially allocated transitions based on neighborhood configuration, slope, and distance from roads and existing settlements.
- A 5 × 5 cell contiguity filter was used to model spatial dependency.

Model validation was performed using the three-map comparison technique [28], comparing the simulated 2023 map with the actual classified 2023 imagery. The model achieved a Kappa Index of Agreement (KIA) > 0.85, indicating high reliability. These indicators were applied to compare the reliability and predictive capability of CA-Markov, providing a robust assessment of their effectiveness in simulating agricultural land-use change in Batu City.

2.7 Overlay with disaster-prone zones

To evaluate land use vulnerability, the simulated 2043 map was overlaid with the disaster-prone area layer from the RTRW Batu City 2022-2042 in Figure 3, and the classification of disasters and their respective spatial extents are provided in Table 1, which includes landslide and flood hazard zones. Overlay analysis quantified the percentage of predicted residential expansion encroaching into high-risk zones, indicating potential spatial conflict between development and environmental safety.

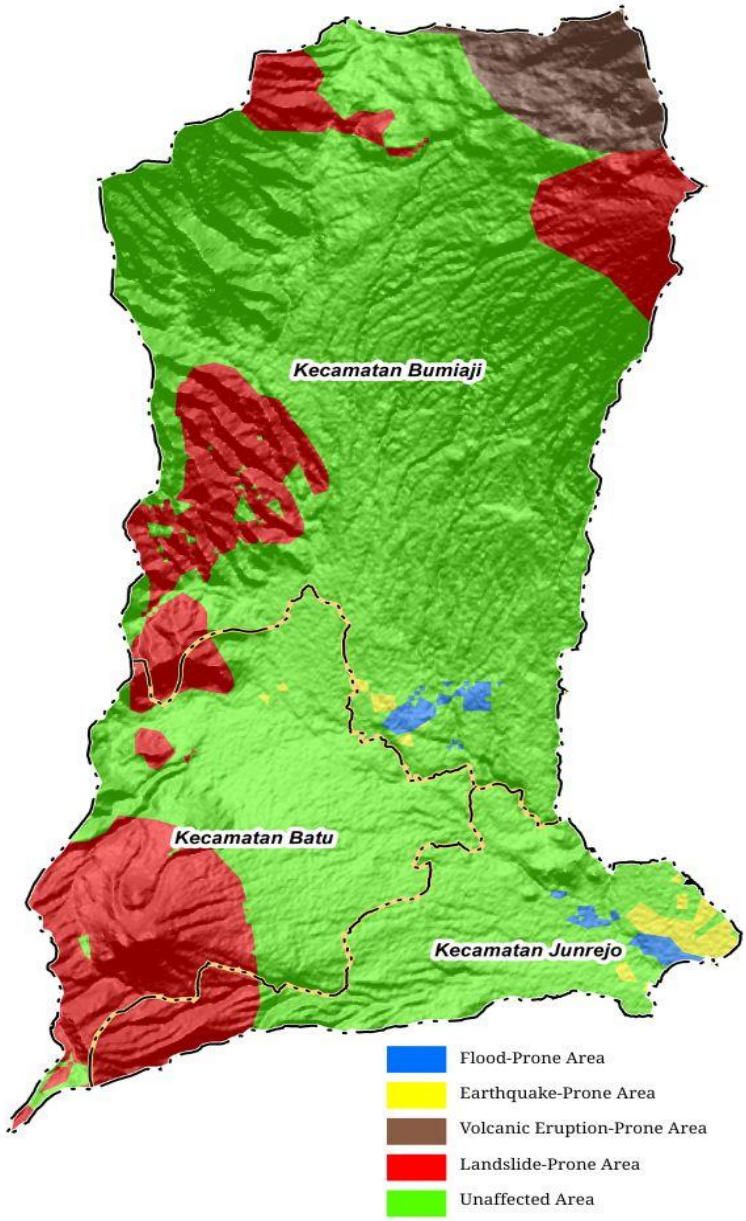

Figure 3. Disaster-prone areas of Batu City

Table 1. The classification of disaster-prone areas in Batu City

Classification of Disaster-Prone Areas in Batu City	Total Areas (Ha)			Total (Ha)	%
	Batu District	Bumiaji District	Junrejo District		
Flood-Prone Area	0.00	85.01	71.87	156.88	0.85
Earthquake-Prone Area	6.72	26.82	147.40	180.94	0.98
Volcanic Eruption-Prone Area	0.00	749.03	0.00	749.03	4.04
Landslide-Prone Area	1425.95	1933.27	398.35	3757.56	20.26
Unaffected Area	2793.35	8970.69	1942.68	13706.72	73.89
Total (Ha)	4226.01	11764.82	2560.30	18551.13	100.00

Source: ArcGIS analysis, 2025

2.8 Analytical framework

All spatial analyses were conducted using ArcGIS 10.8, ENVI 5.6, and TerrSet 2020. Quantitative results were tabulated to determine:

- The rate of agricultural land loss (2013-2023)
- The percentage of residential expansion projected for 2043
- The proportion of new development within hazard zones

The methodological integration of GIS and CA-Markov provides a robust framework to evaluate the dynamics of agricultural land commodification and its implications for disaster-prone urban development in Batu City.

3. RESULTS

Based on spatial analysis using ArcGIS, land use changes in Batu City between 2019 and 2023 reveal a significant shift of built-up and agricultural areas into disaster-prone zones. The overlay between the land use map and the disaster-prone zone map (including landslides, earthquakes, floods, volcanic eruptions, and non-disaster zones) indicates that several types of land use have expanded into areas with moderate to high disaster risk levels.

The analysis shows that settlement areas increased their presence within disaster-prone zones by approximately 9.8%**,** especially in the southern and western parts of Batu City, where topographic slopes exceed 20%. Similarly, agricultural land, particularly dryland and plantation areas, experienced a 7.6% increase within landslide-prone and flood-prone areas. Meanwhile, forest areas declined by about 5.4%, mostly in regions adjacent to agricultural expansion. Shrub and bushlands also decreased slightly (-3.2%), replaced by mixed farming and low-density settlements.

3.1 Settlement area

In contrast, regions categorized as non-disaster zones experienced a decrease in new land conversions, indicating that urban expansion is dominantly occurring in environmentally fragile areas. These patterns demonstrate that urban growth and land use change in Batu City are progressing without adequate spatial control, resulting in greater exposure to multiple natural hazards, including landslides**,** earthquakes, floods, and volcanic activity from Mount Arjuno-Welirang. Table 2 presents the distribution of residential areas in Batu City that intersect with various disaster-prone zones, including floods, earthquakes, volcanic eruptions, and landslides, as well as areas unaffected by disasters. The data were derived from the overlay analysis between the land use map (2019-2023) and the disaster-prone area map based on the Regional Spatial Plan (RTRW) of Batu City and The classification is presented in Table 2. This spatial analysis was conducted using ArcGIS, allowing the identification of residential zones exposed to specific disaster risks.

The findings indicate that a significant portion of residential development has expanded into medium to high disaster-prone areas, particularly those susceptible to landslides and volcanic eruptions, due to the city's topographic and geological characteristics. Meanwhile, only a small proportion of residential land remains in zones categorized as non-disaster areas. This trend reflects the increasing spatial pressure on safe land and highlights the need for better spatial planning and disaster risk mitigation in future urban development.

Based on the table above, the area of disaster-prone residential zones in Batu City shows a gradual increase from 2019 to 2023 and the map presented in Figure 4. In 2019, the total disaster-prone residential area covered 314.91 hectares, or approximately 7.31% of the total residential land, while in 2023 it increased to 367.18 hectares, or 7.37%. Although the percentage increase appears relatively small, this trend indicates a growing risk of disasters affecting residential areas, driven by environmental changes and ongoing urban development. Spatially, Bumiaji District contributes the largest share of disaster-prone residential areas, followed by Batu District and Junrejo District, reflecting the topographical and geological variations that influence disaster vulnerability across the city. Bumiaji District in Batu City emerges as particularly vulnerable, with thirty-two recorded disaster outbreaks and Tulungrejo village is identified as the highest-risk area [1]. Flood susceptibility mapping in Bumiaji District shows moderate risk levels (scoring 90), attributed to high-intensity rainfall and land use changes affecting water infiltration in this mountainous region [8, 29].

Table 2. The classification of disaster-prone areas in Batu City in residential areas

Years	Classification of Disaster-Prone Areas in Batu City	Disaster Prone Area (Ha)			Total Area (Ha)	%
		Batu District	Bumiaji District	Junrejo District		
2019	Flood-Prone Residential Area	0.00	58.09	30.25	88.34	2.05
	Earthquake-Prone Residential Area	3.68	26.82	87.98	118.47	2.75
	Volcanic Eruption-Prone Residential Area	0.00	4.79	0.00	4.79	0.11
	Landslide-Prone Residential Area	67.43	35.89	0.00	103.31	2.40
	Non-Disaster (Unaffected) Residential Area	1800.57	1219.22	976.05	3995.84	92.69
	Total (Ha)	1871.68	1344.81	1094.28	4310.76	100.00

2020	Flood-Prone Residential Area	0.00	68.55	34.47	103.02	2.30
	Earthquake-Prone Residential Area	3.75	26.82	90.35	120.92	2.69
	Volcanic Eruption-Prone Residential Area	0.00	4.31	0.00	4.31	0.10
	Landslide-Prone Residential Area	63.66	39.14	0.00	102.80	2.29
	Non-Disaster (Unaffected) Residential Area	1831.13	1303.09	1021.91	4156.13	92.62
	Total (Ha)	1898.54	1441.90	1146.74	4487.18	100.00
2021	Flood-Prone Residential Area	0.00	69.90	35.88	105.78	2.33
	Earthquake-Prone Residential Area	4.56	26.82	91.11	122.49	2.70
	Volcanic Eruption-Prone Residential Area	0.00	3.49	0.00	3.49	0.08
	Landslide-Prone Residential Area	66.45	35.21	0.00	101.65	2.24
	Non-Disaster (Unaffected) Residential Area	1829.61	1312.71	1061.54	4203.87	92.65
	Total (Ha)	1900.62	1448.13	1188.54	4537.28	100.00
2022	Flood-Prone Residential Area	0.00	70.77	37.67	108.45	2.31
	Earthquake-Prone Residential Area	4.51	26.82	93.02	124.35	2.65
	Volcanic Eruption-Prone Residential Area	0.00	2.99	0.00	2.99	0.06
	Landslide-Prone Residential Area	66.56	39.46	0.00	106.02	2.26
	Non-Disaster (Unaffected) Residential Area	1855.21	1384.35	1117.81	4357.37	92.73
	Total (Ha)	1926.28	1524.39	1248.51	4699.18	100.00
2023	Flood-Prone Residential Area	0.00	73.30	41.00	114.31	2.30
	Earthquake-Prone Residential Area	4.87	26.82	94.32	126.01	2.53
	Volcanic Eruption-Prone Residential Area	0.00	6.07	0.00	6.07	0.12
	Landslide-Prone Residential Area	72.55	48.24	0.00	120.79	2.43
	Non-Disaster (Unaffected) Residential Area	1930.91	1510.28	1171.88	4613.06	92.63
	Total (Ha)	2008.32	1664.70	1307.20	4980.23	100.00

Source: Analysis result, 2025

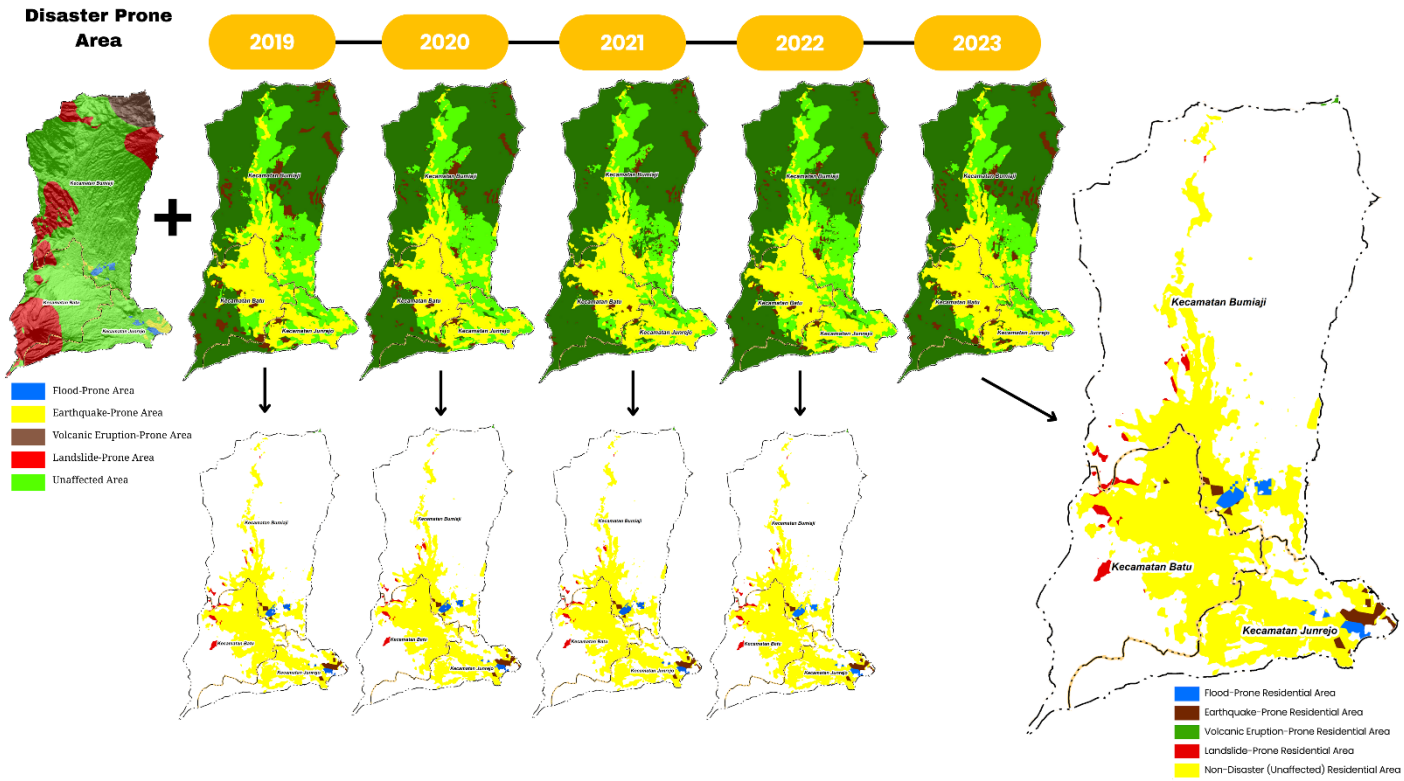

Figure 4. Map of the classification of disaster-prone areas in Batu City in residential areas
Source: ArcGIS analysis, 2025

3.2. Agricultural area

The spatial dynamics of agricultural land in Batu City from 2019 to 2023 demonstrate a gradual but significant shift toward disaster-prone areas. As land demand increases due to urban expansion and land commodification, agricultural activities have begun to occupy zones with higher physical risks, including flood, earthquake, and landslide-prone regions. This phenomenon indicates not only a decrease in the availability of safe agricultural zones but also an increasing pressure on areas that should ideally remain as ecological buffers. The data presented below classify agricultural land use within different types of disaster-prone zones in three districts, Batu, Bumiaji, and Junrejo, during five years, providing insight into how agricultural land expansion intersects with natural hazard exposure.

Table 3 and Figure 5 show a clear trend of agricultural areas increasingly encroaching upon disaster-prone zones. From 2019 to 2023, the percentage of agricultural land located in landslide-prone zones grew steadily, while safe (non-affected) agricultural areas declined from 93.04% to 94.21%, reflecting a gradual yet consistent reduction of secure cultivation space.

Bumiaji District exhibits the most significant concentration of agricultural activity within landslide-prone areas, corresponding to its topographic and geomorphological characteristics dominated by steep slopes. The persistence of this spatial pattern highlights the urgency of implementing stricter land-use regulations and integrating hazard mapping into agricultural planning. Without adequate control, the continued conversion and utilization of risky areas for farming could lead to decreased land productivity and increased vulnerability to natural disasters in the future.

Table 3. The classification of disaster-prone areas in Batu city in agricultural areas

Years	Classification of Disaster-Prone Areas in Batu City	Disaster Prone Areas (Ha)			Total (Ha)	%
		Batu District	Bumiaji District	Junrejo District		
2019	Agricultural Areas Prone to Flood Disasters	0.00	26.86	38.99	65.85	1.71
	Agricultural Areas Prone to Earthquake Disasters	3.04	0.00	59.42	62.46	1.62
	Agricultural Areas Prone to Landslide Disasters	7.27	132.52	0.00	139.79	3.63
	Agricultural Areas Not Affected by Disasters	395.26	2531.13	654.84	3581.22	93.04
	Total (Ha)	405.57	2690.50	753.25	3849.32	100.00
2020	Agricultural Areas Prone to Flood Disasters	0.00	16.44	34.46	50.90	1.37
	Agricultural Areas Prone to Earthquake Disasters	2.97	0.00	56.73	59.71	1.61
	Agricultural Areas Prone to Landslide Disasters	1.72	95.52	0.00	97.24	2.62
	Agricultural Areas Not Affected by Disasters	338.90	2541.26	623.83	3503.99	94.40
	Total (Ha)	343.60	2653.21	715.03	3711.84	100.00
2021	Agricultural Areas Prone to Flood Disasters	0.00	14.27	32.08	46.36	1.29
	Agricultural Areas Prone to Earthquake Disasters	2.16	0.00	55.98	58.14	1.62
	Agricultural Areas Prone to Landslide Disasters	4.73	106.25	0.00	110.97	3.10
	Agricultural Areas Not Affected by Disasters	338.03	2479.26	548.39	3365.69	93.98
	Total (Ha)	344.92	2599.79	636.46	3581.17	100.00
2022	Agricultural Areas Prone to Flood Disasters	0.00	11.44	31.19	42.63	1.35
	Agricultural Areas Prone to Earthquake Disasters	2.21	0.00	53.74	55.96	1.77
	Agricultural Areas Prone to Landslide Disasters	2.54	75.54	0.00	78.08	2.46
	Agricultural Areas Not Affected by Disasters	279.76	2233.26	479.74	2992.76	94.43
	Total (Ha)	284.52	2320.24	564.67	3169.43	100.00
2023	Agricultural Areas Prone to Flood Disasters	0.00	9.77	27.42	37.19	1.19
	Agricultural Areas Prone to Earthquake Disasters	1.85	0.00	52.56	54.41	1.74
	Agricultural Areas Prone to Landslide Disasters	3.90	85.27	0.00	89.16	2.85
	Agricultural Areas Not Affected by Disasters	237.27	2298.74	406.57	2942.57	94.21
	Total (Ha)	243.02	2393.77	486.55	3123.34	100.00

Source: Analysis result, 2025

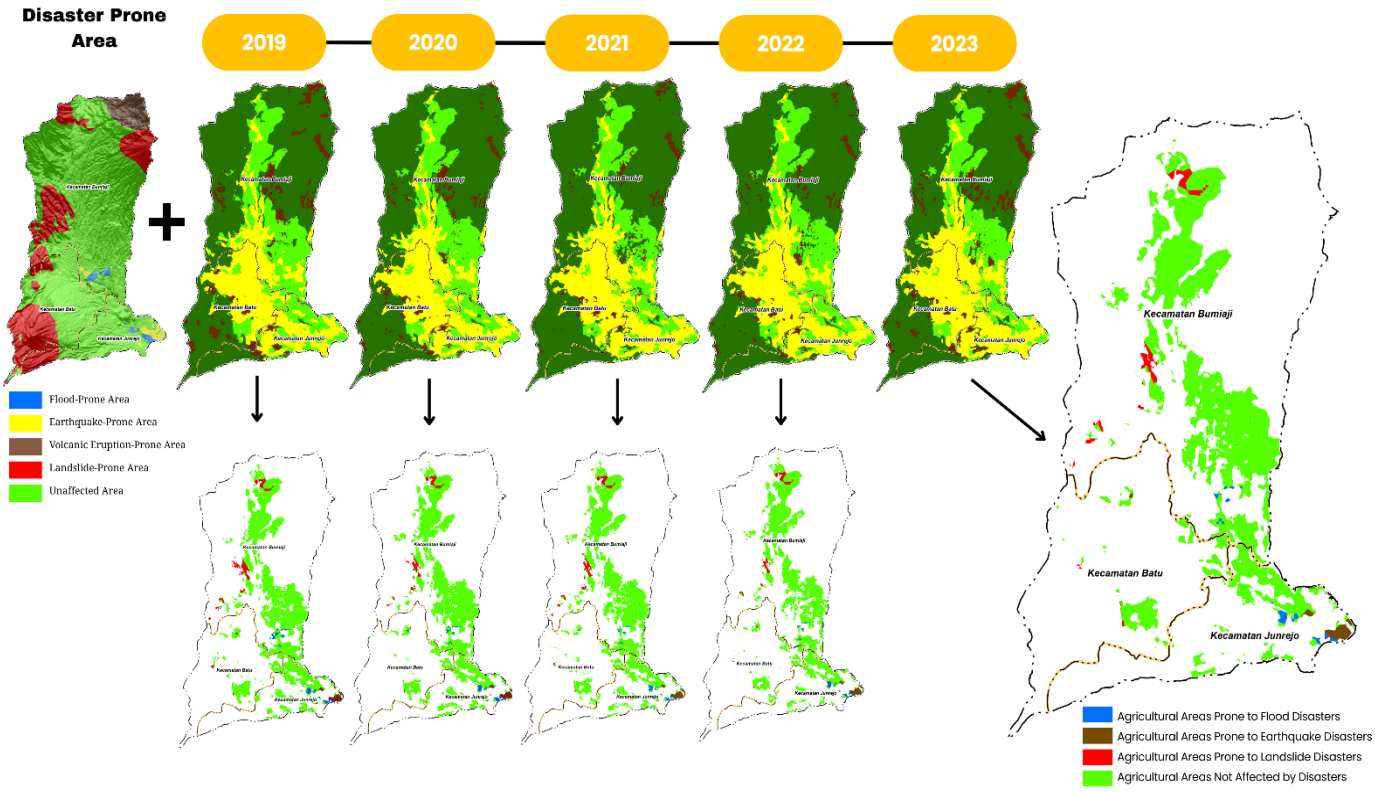

Figure 5. Map of the classification of disaster-prone areas in Batu City in agricultural areas

Source: ArcGis analysis, 2025

Table 4. CA-Markov analysis in disaster-prone areas 2033

CA-Markov Analysis in Disaster-Prone Areas 2033 (Ha)				
Classifications	**Batu District**	**Bumiaji District**	**Junrejo District**	**Total**
Agricultural - Earthquake & Flood	-	-	9.58	9.58
Agricultural - Landslide	3.13	78.38	-	81.51
Agricultural - Save Zone	228.04	1836.74	459.06	2523.84
Agricultural Area - Flood	-	9.64	20.57	30.21
Agricultural Area -Earthquake	1.84	-	58.52	60.37
Forest Area - Flood	-	1.80	3.42	5.22
Forest Area - Landslide	1306.97	1697.24	524.38	3528.60
Forest Area - Landslide & Volcano Eruption	-	232.80	-	232.80
Forest Area - Save Zone	596.70	5075.36	460.61	6132.66
Forest Area - Volcano Eruption	-	377.91	-	377.91
Forest Area -Earthquake	-	-	0.07	0.07
Settlement - Earthquake & Flood	-	8.59	14.97	23.56
Settlement - Landslide	119.24	141.31	-	260.54
Settlement - Landslie & Volcano Eruption	-	57.99	-	57.99
Settlement - Save Zone	2024.33	2042.95	1327.07	5394.36
Settlement - Volcano Eruption	-	43.97	-	43.97
Settlement Area - Earthquake	4.97	26.73	101.32	133.01
Settlement Area - Flood	-	64.87	28.26	93.13
Shrubland - Earthquake	-	-	0.39	0.39
Shrubland - Landslide	28.59	62.36	0.15	91.11
Shrubland - Landslide & Volcano Eruption	-	57.54	-	57.54
Shrubland - Save Zone	27.08	170.53	56.75	254.37
Shrubland - Volcano Eruption	-	13.73	-	13.73
Shrubland Area - Flood	-	0.11	-	0.11
Total	**4340.90**	**12000.56**	**3065.13**	**19406.59**

Source: Analysis result, 2025

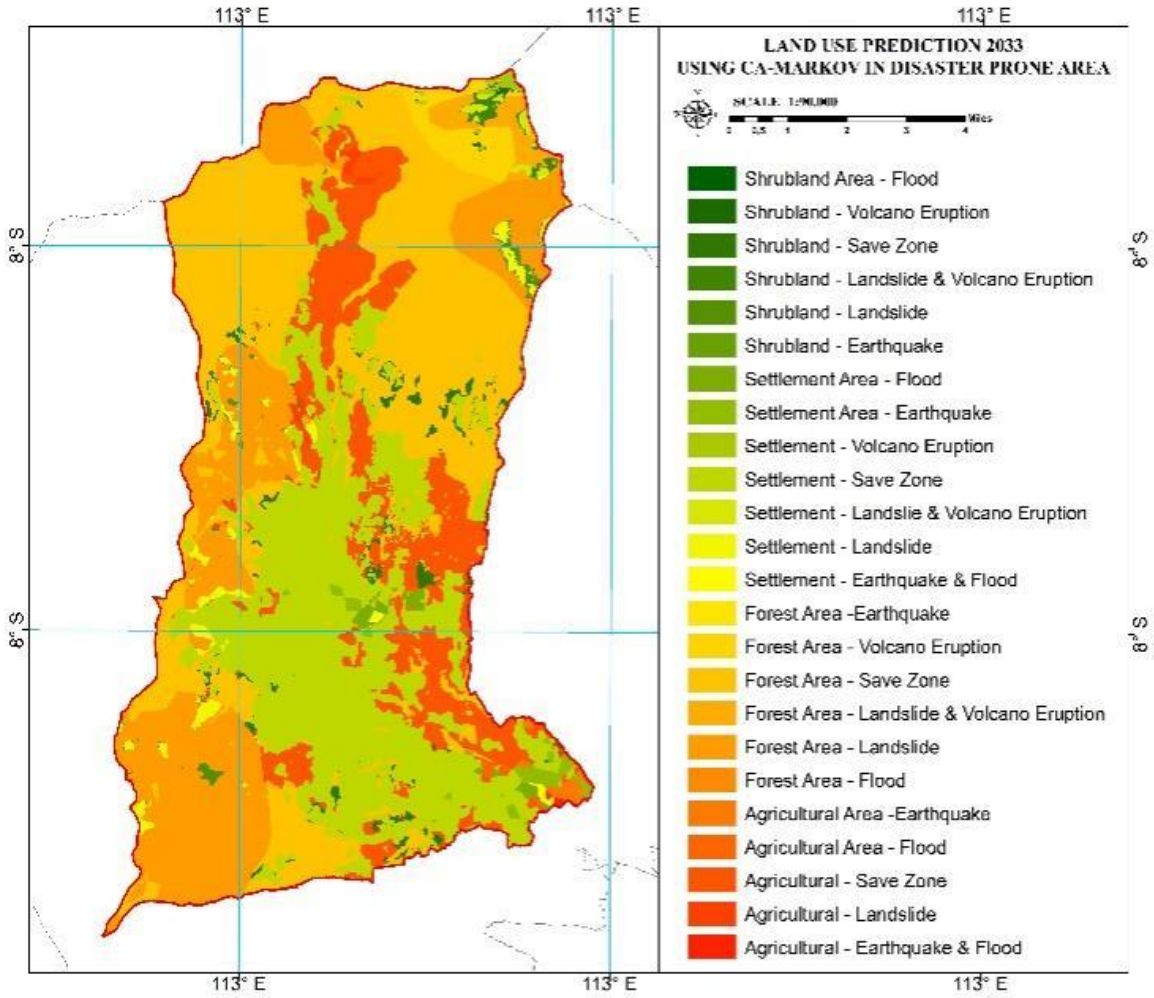

Figure 6. Map CA-Markov analysis in disaster-prone areas 2033

3.3 CA-Markov analysis in disaster-prone areas 2033

The prediction of land use distribution for the year 2033 based on the CA-Markov model presents a spatial projection of land transformation patterns in disaster-prone zones of Batu City. This model integrates transition probabilities from past land-use changes and spatial autocorrelation to estimate future land cover under disaster risk scenarios. The analysis overlays the projected land-use map with the official disaster-prone map, highlighting the potential intersection between built-up, agricultural, forested, and shrubland areas with zones susceptible to floods, landslides, earthquakes, and volcanic eruptions.

The overall predicted land area exposed to disaster-prone zones in Batu City by 2033 in Table 4 and Figure 6 reaches 19,406.59 hectares, distributed across three districts: Batu (4,340.90 ha or 22.38%), Bumiaji (12,000.56 ha or 61.86%), and Junrejo (3,065.13 ha or 15.78%). Among all land-use classes, forest areas contribute the largest portion of disaster-prone coverage, accounting for 10,277.26 ha (52.96%), followed by settlement areas (6,306.56 ha or 32.50%), agricultural areas (2,705.51 ha or 13.94%), and shrubland (817.26 ha or 4.21%). The "save zone" categories across all land uses dominate the classification, indicating potential regions less affected by natural disasters. For instance, forest save zones cover 6,132.66 ha (31.6%), while settlement save zones occupy 5,394.36 ha (27.8%), reflecting areas with lower disaster vulnerability but still within the model's predictive framework. However, the forest landslide area remains the most significant disaster-related classification, reaching 3,528.60 ha (18.17%), primarily concentrated in Bumiaji District (1,697.24 ha) and Batu District (1,306.97 ha). The agricultural sector also shows substantial exposure to landslides (81.51 ha) and earthquakes (60.37 ha), with minor vulnerability to floods (30.21 ha). Settlement areas are notably exposed to both earthquake (133.01 ha) and flood hazards (93.13 ha), especially in the Junrejo District, where rapid urban expansion intersects with unstable slopes and river corridors. Meanwhile, shrubland areas show minimal but significant exposure to landslide and volcanic eruption risks, totaling 219.38 ha (1.13%).

The spatial overlay between the CA-Markov 2033 predicted land-use map and the disaster-prone map reveals potential conflicts between land development and environmental vulnerability. The prediction suggests that without strict land-use control and enforcement of spatial planning regulations (RTRW), a significant portion of agricultural and settlement areas will continue expanding toward landslide-prone and flood-prone zones, particularly in Bumiaji and Junrejo districts. These findings underline the urgent need for integrated spatial planning that considers disaster risk reduction as a key component of urban and regional development. The CA-Markov model provides a quantitative basis for formulating anticipatory policies, such as zoning regulations, slope stabilization measures, and the conservation of forested buffers in upper watersheds.

3.4 CA-Markov analysis in disaster-prone areas 2043

The CA–Markov land use simulation for 2043 projects future spatial transformations in Batu City by integrating Markov chain transition probabilities with spatial contiguity through cellular automata. This model provides a dynamic prediction of land-use distribution under continuous development pressure and environmental constraints. By overlaying the 2043 land-use prediction with Batu City's disaster-prone areas, the analysis identifies potential spatial overlaps between land-use categories and zones exposed to geological and hydrometeorological hazards such as landslides, floods, earthquakes, and volcanic eruptions.

Table 5. CA-Markov analysis in disaster-prone areas 2043

CA-MARKOV Disaster Prone Areas 2043 (Ha)				
Classifications	**Batu District**	**Bumiaji District**	**Junrejo District**	**Total**
Agricultural - Landslide	-	11.99	-	11.99
Agricultural - Save Zone	0.94	22.81	-	23.75
Forest Area - Earthquake	1.36	-	0.05	1.41
Forest Area - Flood	-	5.18	3.41	8.60
Forest Area - Landslide	1311.25	1696.81	524.42	3532.48
Forest Area - Save Zone	611.83	5097.87	459.21	6168.92
Forest Area - Volcano Eruption	-	357.00	-	357.00
Forest Area - Volcano Eruption & Landslide	-	232.54	-	232.54
Settlement - Earthquake	5.45	26.73	160.55	192.73
Settlement - Earthquake & Flood	-	8.59	24.69	33.28
Settlement - Flood	-	71.24	48.92	120.16
Settlement - Landslide	147.22	264.84	0.43	412.50
Settlement - Save Zone	2263.88	3967.12	1846.49	8077.49
Settlement - Volcano Eruption	-	79.15	-	79.15
Settlement - Volcano Eruption & Landslide	-	116.07	-	116.07
Shrubland - Landslide	0.27	6.83	-	7.10
Shrubland - Save Zone	0.42	40.64	-	41.06
Total	**4342.62**	**12005.41**	**3068.18**	**19416.22**

Source: Analysis result, 2025

The total predicted land area in Table 5 and the map in Figure 7 within disaster-prone zones in Batu City by 2043 is 19,416.22 hectares, showing only a slight increase of 0.05% compared to the 2033 projection (19,406.59 ha). Spatially, the distribution remains concentrated in Bumiaji District (12,005.41 ha or 61.86%), followed by Batu District (4,342.62 ha or 22.37%), and Junrejo District (3,068.18 ha or 15.78%). This pattern indicates that disaster-prone expansion and land-use interaction are relatively stable over the projection period, suggesting limited but continuous development within sensitive zones. Among land-use categories, forest areas continue to dominate disaster-prone coverage with 8,401.95 ha

(43.26%), followed by settlement areas (9,308.88 ha or 47.94%), agricultural land (35.74 ha or 0.18%), and shrubland (48.16 ha or 0.25%). The remaining 621.49 ha (3.20%) belong to mixed categories such as volcano eruption and landslide combinations. The forest save zone still accounts for the largest safe-area coverage (6,168.92 ha or 31.77% of total), but a notable concern arises from the forest landslide-prone area, which remains substantial at 3,532.48 ha (18.18%), especially in Bumiaji District (1,696.81 ha) and Batu District (1,311.25 ha). Settlement areas also exhibit continued expansion into hazard-prone zones, particularly into landslide-prone areas (412.50 ha or 2.12%), earthquake zones (192.73 ha or 0.99%), and flood-prone zones (120.16 ha or 0.62%). The increasing spread of urban areas into risk-prone regions reflects the high development pressure and limited available land within safer zones, especially in Junrejo District, where residential areas intersect with flood and earthquake hazard lines. The overlay analysis between the CA-Markov 2043 predicted land-use map and disaster-prone areas reveals that, while the overall extent of at-risk land remains nearly constant from 2033 to 2043, the composition within these areas shifts toward greater urban and settlement intensity. Forest zones, although still dominant in total area, exhibit gradual fragmentation due to the encroachment of built-up land near slopes and water bodies. This spatial pattern underscores the continuing tension between urban expansion and environmental vulnerability. Spatially, Bumiaji District remains the most critical area due to its high exposure to multiple hazard types, particularly landslides and volcanic activity, while Junrejo District faces growing exposure to floods and earthquakes due to rapid urbanization. Batu District, though smaller in area, plays a strategic ecological role as a buffer zone that supports forest conservation and reduces downstream flood risk. The results emphasize the importance of integrating disaster risk reduction (DRR) principles into spatial planning and land-use management. Land-use policies should prioritize slope stabilization, forest preservation, and settlement control in hazard-prone regions. The CA–Markov predictive framework provides valuable spatial evidence to guide proactive urban planning, allowing stakeholders to anticipate future land conflicts and mitigate potential disaster impacts.

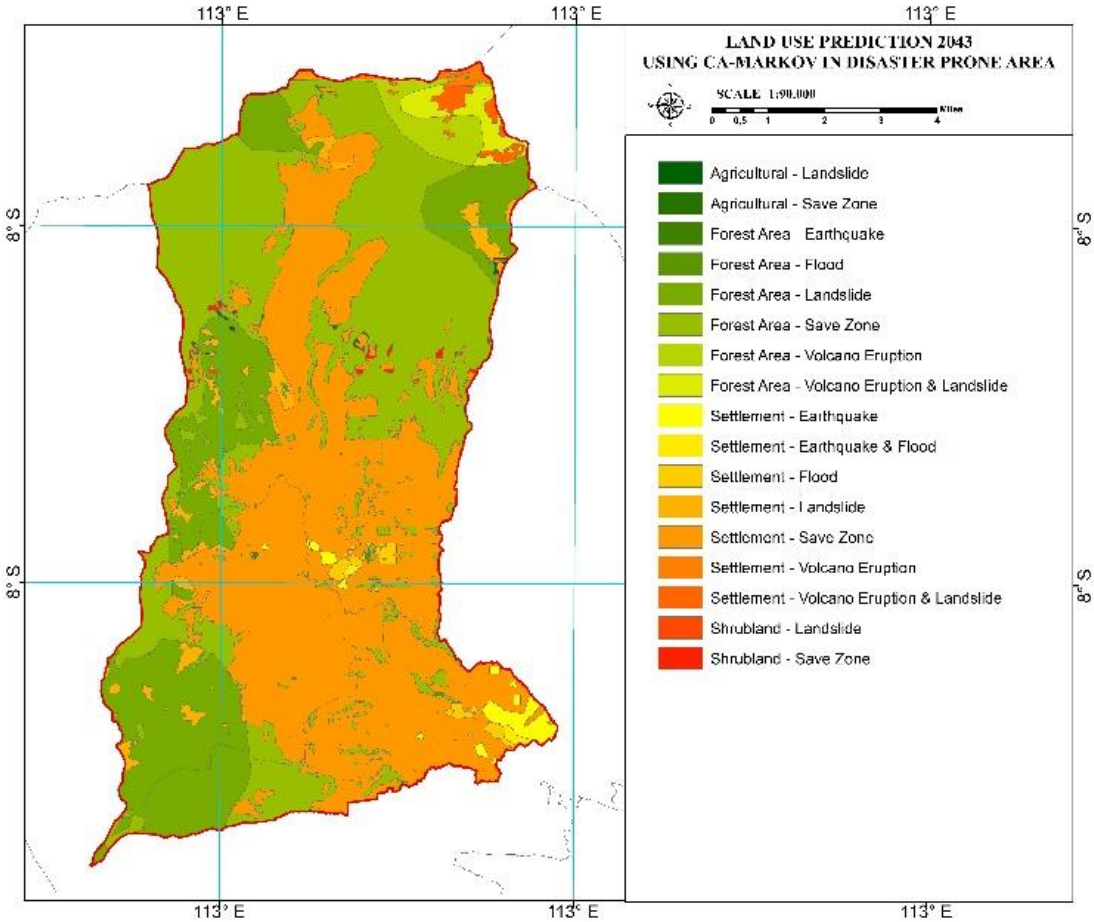

Figure 7. Map CA-Markov analysis in disaster-prone areas 2043

3.5 The validation of CA-Markov analysis

The observed land use change simulation with the CA-Markov model reveals a highly dependable function for simulating both spatial and temporal transitions in Batu City. The Markov chain model calculates the probability of land use change based on past patterns, while the cellular automata help represent spatial allocation according to a neighborhood effect. The combination of the two is vital, as it allows the model to scale the number of pixels changed while still representing spatial aspects of land use change. In Figures 8 and 9, the overall validation results reveal metric outcomes of Kstandard of 0.8889 and Kno of 0.8973, indicating a strong agreement of land use simulation and observed land use data. The Klocation metric of 0.9256 further indicates the user's acceptable prediction of the spatial allocation of land conversion, specifically for the case of agricultural land conversion into built-up. The final metric, an AgreeGridcell

value of 0.6161, indicates that the simulation accounted for more than half the observed changes when evaluated at grid-cell size, but there is a measurable amount of spatial agreement (0.0495).

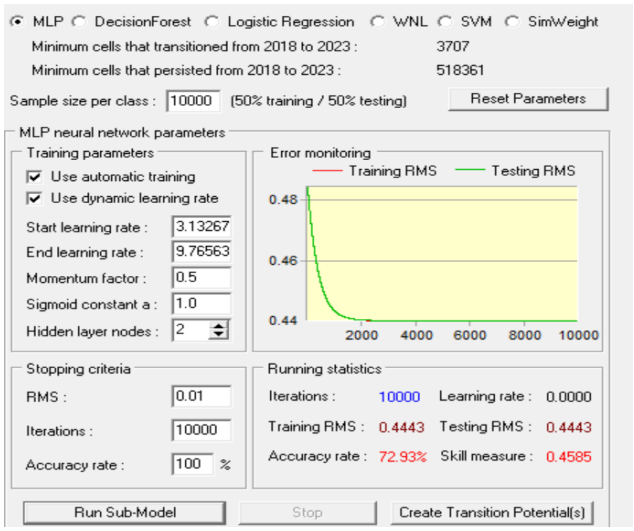

Figure 8. Prediction CA-Markov analysis

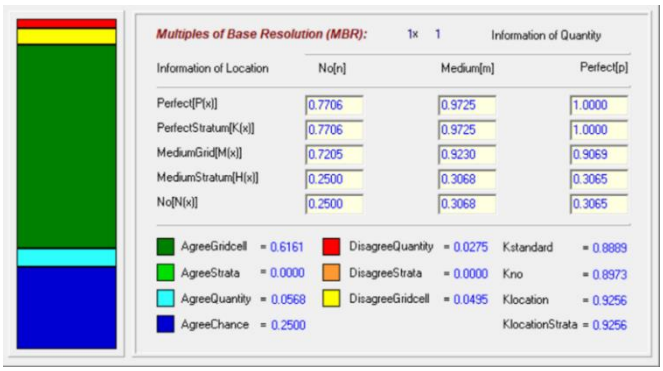

Figure 9. Validation of CA-Markov analysis

4. CONCLUSION

The analysis reveals that Batu City has experienced a continuous shift of both residential and agricultural land into disaster-prone areas between 2019 and 2023, driven primarily by rapid urbanization and land commodification. Residential expansion increased by about 9.8% within hazard zones, while agricultural land encroachment into landslide and flood-prone regions rose by 7.6%, highlighting the growing spatial overlap between development and environmental risk. This indicates that urban growth in Batu City is occurring without sufficient spatial control, reducing ecological buffers and increasing vulnerability to natural disasters. Therefore, integrating predictive modeling such as CA-Markov with disaster-risk mapping is essential to guide more sustainable, risk-sensitive urban planning and land-use policies in the future.

REFERENCES

[1] Amiruddin, L., Rozalinna, G.M. (2020). Participatory mapping for disasters in Tulungrejo village, Bumiaji sub-district, Batu City. Jurnal Partisipatoris, 2(1): 19-30. https://doi.org/10.22219/jp.v2i1.11743

[2] Jungalwalla, N. (1968). Urbanization and health. Israel Journal of Medical Sciences, 4(3): 532-543. https://doi.org/10.4038/jccpsl.v14i1.2941

[3] Kohlhase, J.E. (2013). The new urban world 2050: Perspectives, prospects and problems. Regional Science Policy & Practice, 5(2): 153-166. https://doi.org/10.1111/rsp3.12001

[4] Schiavina, M., Melchiorri, M., Corbane, C., Freire, S., Batista e Silva, F. (2022). Built-up areas are expanding faster than population growth: Regional patterns and trajectories in Europe. Journal of Land Use Science, 17(1): 591-608. https://doi.org/10.1080/1747423X.2022.2055184

[5] Liu, X., Huang, Y., Xu, X., Li, X., et al. (2020). High-spatiotemporal-resolution mapping of global urban change from 1985 to 2015. Nature Sustainability, 3(7): 564-570. https://doi.org/10.1038/s41893-020-0521-x

[6] Wei, Y.D., Ewing, R. (2018). Urban expansion, sprawl and inequality. Landscape and Urban Planning, 177: 259-265. https://doi.org/10.1016/j.landurbplan.2018.05.021

[7] Hidayat, S.I., Rofiqoh, L.L. (2020). Analysis of agricultural land function transfer in Kediri Regency. Jurnal Social Economic of Agriculture, 9(1): 59. https://doi.org/10.26418/j.sea.v9i1.40646

[8] Paddiyatu, N., Umar, F., Zainuddin, S., Arista, M.A.Y. (2023). Model perkembangan permukiman berbasis cellular automata di kabupaten takalar. Jurnal Pembangunan Wilayah Dan Kota, 19(3): 409-421. https://doi.org/10.14710/pwk.v19i3.45639

[9] Prayitno, G., Subagiyo, A., Kusriyanto, R.L. (2020). Conversion of agricultural land to non-agricultural use in Batu City, Indonesia. https://doi.org/10.31764/GEOGRAPHY.V8I2.2653

[10] Yaro, J.A. (2012). Re-inventing traditional land tenure in the era of land commoditization: Some consequences in periurban northern Ghana. Geografiska Annaler: Series B, Human Geography, 94(4): 351-368. https://doi.org/10.1111/geob.12003

[11] Hasibuan, H.C., Rahayu, S. (2017). Kesesuaian lahan permukiman pada kawasan rawan bencana tanah longsor di Kabupaten Temanggung. Teknik PWK (Perencanaan Wilayah Kota), 6(4): 242-256.

[12] Sudarto, A., Utami, W. (2021). Analysis of settlement location availability based on landslide mitigation. Jurnal Pengembangan Kota, 9(2): 166-179. https://doi.org/10.14710/jpk.9.2.166-179

[13] Van der Werff, H., Van der Meer, F. (2016). Sentinel-2A MSI and Landsat 8 OLI provide data continuity for geological remote sensing. Remote Sensing, 8(11): 883. https://doi.org/10.3390/rs8110883

[14] Yang, X., Zhao, S., Qin, X., Zhao, N., Liang, L. (2017). Mapping of urban surface water bodies from Sentinel-2 MSI imagery at 10 m resolution via NDWI-based image sharpening. Remote Sensing, 9(6): 596. https://doi.org/10.3390/rs9060596

[15] Riestu, I.M., Hidayat, H. (2023). Landslide susceptibility mapping using random forest algorithm and its correlation with land use in Batu City, Jawa Timur. IOP Conference Series: Earth and Environmental Science, 1127(1): 012017. https://doi.org/10.1088/1755-1315/1127/1/012017

[16] Chavez Jr, P.S. (1988). An improved dark-object

subtraction technique for atmospheric scattering correction of multispectral data. Remote Sensing of Environment, 24(3): 459-479. https://doi.org/10.1016/0034-4257(88)90019-3
[17] Baboo, S.S., Devi, M.R. (2011). Geometric correction in recent high resolution satellite imagery: A case study in Coimbatore, Tamil Nadu. International Journal of Computer Applications, 14(1): 32-37. https://doi.org/10.5120/1808-2324
[18] Dave, C.P., Joshi, R., Srivastava, S. (2015). A survey on geometric correction of satellite imagery. International Journal of Computer Applications, 116(5): 24-27. https://doi.org/10.5120/20389-2655
[19] Derse, M.A., Alphan, H. (2024). Atmospheric and radiometric normalization of satellite images for landscape-level environmental monitoring: The case of the Mediterranean Region. Journal of Architectural Sciences and Applications, 9(1): 620-633. https://doi.org/10.30785/mbud.1446007
[20] Studley, H., Weber, K.T. (2011). Comparison of image resampling techniques for satellite imagery. Final Report: Assessing Post-Fire Recovery of Sagebrush-Steppe Rangelands in Southeastern Idaho, 252: 185-196. https://giscenter.isu.edu/research/Techpg/nasa_postfire/pdf/Ch15.pdf.
[21] Le Trinh, H., Le, H.T.T., Le, L.D., Nguyen, L.T. (2021). A development of the enhanced built-up and Bareness Index (EBBI) based on combination of multi-resolution landsat 8 and sentinel 2 MSI images. Journal of Mining and Earth Sciences, 62(1): 1-9. https://doi.org/10.46326/JMES.2021.62(1).01
[22] Xi, Y., Thinh, N.X., Li, C. (2019). Preliminary comparative assessment of various spectral indices for built-up land derived from Landsat-8 OLI and sentinel-2A MSI imageries. European Journal of Remote Sensing, 52(1): 240-252. https://doi.org/10.1080/22797254.2019.1584737
[23] Manandhar, R., Odeh, I.O., Ancev, T. (2009). Improving the accuracy of land use and land cover classification of Landsat data using post-classification enhancement. Remote Sensing, 1(3): 330-344. https://doi.org/10.3390/rs1030330
[24] Murtaza, K.O., Romshoo, S.A. (2014). Determining the suitability and accuracy of various statistical algorithms for satellite data classification. International Journal of Geomatics and Geosciences, 4(4): 585-599.
[25] Rwanga, S., Ndambuki, J. (2017). Accuracy assessment of land use/land cover classification using remote sensing and GIS. International Journal of Geosciences, 8(4): 611-622. https://doi.org/10.4236/ijg.2017.84033
[26] Foody, G.M. (2002). Status of land cover classification accuracy assessment. Remote Sensing of Environment, 80(1): 185-201. https://doi.org/10.1016/S0034-4257(02)00034-0
[27] Umrikar, B., Patil, M., Desai, C.G. (2011). Application of cellular automata technique for prediction of growth pattern through Java programming. https://www.researchgate.net/publication/280239897_Application_of_cellular_automata_technique_for_prediction_of_growth_pattern_through_Java_programming.
[28] Pontius, R.G., Millones, M. (2011). Death to Kappa: Birth of quantity disagreement and allocation disagreement for accuracy assessment. International Journal of Remote Sensing, 32(15): 4407-4429. https://doi.org/10.1080/01431161.2011.552923
[29] Muzaqi, A.H., Ambulanto, T. (2020). Mapping of strategic issues in the preparation of the Malang City regional medium-term development plan (RPJMD) document. Jurnal Mediasosian: Jurnal Ilmu Sosial Dan Administrasi Negara, 4(2): 172-192. https://doi.org/10.30737/mediasosian.v4i2.1201